

Coherent nonlinear optical response of graphene in the quantum Hall regime

H.K. Avetissian and G.F. Mkrtchian

Centre of Strong Fields Physics, Yerevan State University, 1 A. Manukian, Yerevan 0025, Armenia

We study nonlinear optical response of graphene in the quantum Hall regime to an intense laser pulse. In particular, we consider harmonic generation process. We demonstrate that the generalized magneto-optical conductivity of graphene on the harmonics of a strong pump laser radiation has a characteristic Hall plateaus feature. The plateaus heights depend on the laser intensity and broadening of Landau levels, so that are not quantized exactly. This nonlinear effect remains robust against the significant broadening of Landau levels. We predict realization of an experiment through the observation of the third harmonic signal and nonlinear Faraday effect, which are within the experimental feasibility.

PACS numbers: 73.43.-f, 78.67.Wj, 78.47.jh, 42.50.Hz

I. INTRODUCTION

Graphene, a single sheet of carbon atoms in a honeycomb 2D lattice, has attracted a tremendous interest since its experimental realization.^{1,2} Graphene possesses several exotic features because of a linear energy dispersion law around the two nodal points K and K' in the Brillouin zone. Due to its unique electronic band structure and specific electromagnetic properties (in particular, high degree of nonlinearity³), graphene is widely considered as a promising material in various nonlinear optical applications. Hence, it is of actual interest to study graphene fundamental physics in the presence of an electric, magnetic, and/or optical fields. When a static magnetic field (uniform) is applied perpendicular to the graphene plane, the electron energy is quantized forming nonequidistant Landau levels (LL). For the massless Dirac quasiparticles extra LL appears with zero energy shared by both electrons and holes without an energy gap. As a consequence, in the graphene the anomalous half-integer quantum Hall effect (QHE) takes place.⁴⁻⁷ This differs strongly from a integer QHE in conventional two-dimensional electron gas.⁸ As is well known, in the static QHE the Hall resistance is quantized into plateaus, which is a topological phenomenon.⁹ Thus, being topologically protected it is robust against details of the disorder. Topological analysis of the QHE in graphene¹⁰ shows that the zero-mass Dirac QHE persists up to the van Hove singularities. Optical response of the graphene QHE system has been studied by different groups. Optical conductivity of graphene QHE system with the different aspects have been studied in Refs. [11–17]. Ultrafast carrier dynamics and carrier multiplication in Landau-quantized graphene have been investigated in Refs. [18,19]. In Refs. [16,20] tunable graphene-based laser on the Landau levels in the terahertz regime have been proposed. As was shown in Ref. [11] the plateau structure in the QHE in 2DEG and in graphene is retained, up to significant degree of disorder, even in the ac (THz) regime, although the heights of the plateaus are no longer quantized. While most of the works have concentrated on static or linear optical prop-

erties of the graphene QHE system, one direction that has not been fully explored is the nonlinear response of Landau-quantized graphene to a strong laser radiation, which is the purpose of the present study. Note that in the absence of the magnetic field graphene is an effective material for multiphoton interband excitation, wave mixing, and harmonic generation.^{3,21} Thus, in the magnetic field due to peaks in the density of states one can expect enhancement of the harmonic radiation power.

In the graphene QHE system, wave-particle interaction can be characterized by the dimensionless parameter $\chi = eE_0l_B/\hbar\omega$, which represents the work of the wave electric field E_0 on the magnetic length $l_B = \sqrt{\hbar c/eB}$ (e is the elementary charge, \hbar is Planck's constant, c is the light speed in vacuum, and B is the magnetic field strength) in units of photon energy $\hbar\omega$. Depending on the value of this parameter χ , one can distinguish three different regimes in the wave-particle interaction process. Thus, $\chi \ll 1$ corresponds to the one-photon interaction regime, $\chi \gg 1$ corresponds to the static field limit, and $\chi \sim 1$ to the multiphoton interaction regime. In this paper we consider just multiphoton interaction regime and look for features in the harmonic spectra of the laser driven graphene. Accordingly, the time evolution of the considered system is found using a nonperturbative numerical approach, revealing that the generalized magneto-optical conductivity of graphene on the harmonics of a strong pump laser radiation in the quantum Hall regime has a characteristic Hall plateaus feature. The plateaus heights are not quantized exactly and depend on the laser intensity and broadening of Landau levels. The effect remains robust against a significant broadening of Landau levels and takes place for wide range of intensities and frequencies of a pump wave.

The paper is organized as follows. In Sec. II the Hamiltonian which governs the quantum dynamics of considered process and the set of equations for a single-particle density matrix are formulated. In Sec. III, we numerically solve obtained equations and consider coherent nonlinear optical response of graphene in the quantum Hall regime on the fundamental harmonic with limiting linear case and on the third harmonic of an incident wave.

Finally, conclusions are given in Sec. IV.

II. BASIC MODEL AND EVOLUTIONARY EQUATION FOR DENSITY MATRIX

We begin our study with construction of the Hamiltonian which governs the quantum dynamics of considered process. The graphene sheet is taken in the xy plane ($z = 0$) and a uniform static magnetic field is applied in the perpendicular direction. A plane linearly polarized (along the x axis) quasimonochromatic electromagnetic radiation of carrier frequency ω and slowly varying envelope $E_0(t)$ interacts with the such system. To avoid nonphysical effects semi-infinite pulses with smooth turn-on, in particular, with hyperbolic tangent $E_0(t) = E_0 \tanh(t/\tau_r)$ envelope is considered. Here the characteristic rise time τ_r is chosen to be $\tau_r = 20\pi/\omega$. We consider the case of interaction when the wave propagates in the perpendicular direction to the graphene sheet to exclude the effect of the wave magnetic field.³ Under these circumstances the single-particle Hamiltonian of graphene QHE system in the presence of a uniform time-dependent electric field

$$E(t) = E_0(t) \cos \omega t \quad (1)$$

reads:

$$\mathcal{H}_s = \hbar\omega_B \begin{pmatrix} 0 & \hat{a} \\ \hat{a}^\dagger & 0 \end{pmatrix} + \left[\hat{I} \frac{e l_B E(t)}{\sqrt{2}} (\hat{b} + i\hat{a}) + \text{h.c.} \right]. \quad (2)$$

Here $\omega_B = \sqrt{2}v_F/l_B$ plays the role of the cyclotron frequency, v_F is the Fermi velocity, and \hat{I} is the identity matrix. For the interaction Hamiltonian we use a length gauge describing the interaction by the potential energy. The ladder operators \hat{a} and \hat{a}^\dagger describe quantum cyclotron motion, while \hat{b} and \hat{b}^\dagger correspond to guiding center motion. These ladder operators satisfy the usual commutation relations $[\hat{a}, \hat{a}^\dagger] = 1$ and $[\hat{b}, \hat{b}^\dagger] = 1$. The Hamiltonian is applicable near the K point in the Brillouin zone. For the considered model there are no intervalley transitions and the valley index, as well as spin index will be skipped. They will be incorporated into the consideration via the spin g_s and valley g_v degeneracy factors.

The single free particle Hamiltonian, that is the first term in Eq. (2) can be diagonalized analytically.⁷ The wave function and energy spectrum are given by

$$|\psi_{n,m}\rangle = \sqrt{(1 + \delta_{n,0})/2} \begin{pmatrix} \text{sgn}(n)| |n| - 1, m\rangle \\ | |n|, m\rangle \end{pmatrix}, \quad (3)$$

$$\varepsilon_n = \text{sgn}(n) \hbar\omega_B \sqrt{|n|}. \quad (4)$$

Here $| |n|, m\rangle = | |n|\rangle \otimes |m\rangle$, with $| |n|\rangle$ and $|m\rangle$ being the harmonic oscillator wave functions. The eigenstates (3) are defined by the quantum numbers $n = 0, \pm 1, \dots$

and $m = 0, 1, \dots$. Here n is the LL index – for an electron $n > 0$ and for a hole $n < 0$. The extra LL with $n = 0$ is shared by both electrons and holes. The LLs are degenerate upon second quantum number m with the large degeneracy factor $N_B = \mathcal{S}/2\pi l_B^2$ which equals the number of flux quanta threading the 2D surface \mathcal{S} occupied by the electrons. The terms $\sim \hat{a}E(t)$ in the Hamiltonian (2) describe transitions between LLs, while the terms $\sim \hat{b}E(t)$ describe transitions within the same LL. These transitions can be excluded from the consideration by the appropriate choice of Dirac states for the construction of the carrier quantum field operators. Expanding the fermionic field operator

$$|\widehat{\Psi}\rangle = \sum_{n,m} \hat{a}_{n,m} |\widetilde{\psi}_{n,m}\rangle \quad (5)$$

over the dressed states

$$|\widetilde{\psi}_{n,m}\rangle = \exp \left[-\frac{i}{\hbar} \frac{e l_B}{\sqrt{2}} \int_0^t E(t') dt' (\hat{b}^\dagger + \hat{b}) \right] |\psi_{n,m}\rangle, \quad (6)$$

the Hamiltonian of the system in the second quantization formalism

$$\widehat{H} = \langle \widehat{\Psi} | \mathcal{H}_s | \widehat{\Psi} \rangle$$

can be presented in the form:

$$\begin{aligned} \widehat{H} = & \sum_{n=-\infty}^{\infty} \sum_{m=0}^{N_B-1} \varepsilon_n \hat{a}_{n,m}^\dagger \hat{a}_{n,m} \\ & + \sum_{n,n'=-\infty}^{\infty} \sum_{m=0}^{N_B-1} E(t) \mathcal{D}_{n,n'} \hat{a}_{n,m}^\dagger \hat{a}_{n',m}, \end{aligned} \quad (7)$$

where $\hat{a}_{n,m}^\dagger$ and $\hat{a}_{n,m}$ are, respectively, the creation and annihilation operators for a carrier in a LL state, and $\mathcal{D}_{n,n'}$ is the dipole moment operator:

$$\mathcal{D}_{n,n'} = \frac{i e l_B}{2\sqrt{2}} \left[\varkappa_{n,n'} \delta_{|n|,|n'|+1} + \varkappa_{n',n} \delta_{|n|,|n'|-1} \right] \frac{\hbar\omega_B}{\varepsilon_{n'} - \varepsilon_n}, \quad (8)$$

where $\varkappa_{n,n'} = \text{sgn}(n) \sqrt{1 + \delta_{n',0}}$. Then we will pass to Heisenberg representation where operators obey the evolution equation

$$i\hbar \frac{\partial \widehat{L}}{\partial t} = [\widehat{L}, \widehat{H}]$$

and expectation values are determined by the initial density matrix \widehat{D} : $\langle \widehat{L} \rangle = \text{Sp}(\widehat{D} \widehat{L})$. In order to develop microscopic theory of the nonlinear interaction of the graphene QHE system with a strong radiation field, we need to solve the Liouville-von Neumann equation for the single-particle density matrix

$$\rho(n_1, m_1; n_2, m_2, t) = \langle \hat{a}_{n_2, m_2}^\dagger(t) \hat{a}_{n_1, m_1}(t) \rangle. \quad (9)$$

For the initial state of the graphene quasiparticles we assume an ideal Fermi gas in equilibrium. According to

the latter, the initial single-particle density matrix will be diagonal, and we will have the Fermi-Dirac distribution:

$$\rho(n_1, m_1; n_2, m_2, 0) = \rho_F(n_1) \frac{\delta_{n_1, n_2} \delta_{m_1, m_2}}{1 + \exp\left(\frac{\varepsilon_{n_1} - \varepsilon_F}{T}\right)}, \quad (10)$$

$$\rho_F(n_1) = \frac{1}{1 + \exp\left(\frac{\varepsilon_{n_1} - \varepsilon_F}{T}\right)}. \quad (11)$$

Including in Eq. (10) quantity ε_F is the Fermi energy, T is the temperature in energy units. As is seen from the interaction term in the Hamiltonian (7) quantum number m is conserved: $\rho(n_1, m_1; n_2, m_2, t) = \rho_{n_1, n_2}(t) \delta_{m_1, m_2}$. To include the effect of the LLs broadening we will assume that it is caused by the disorder described by randomly placed scatterers. When the range of the random potential is larger than the lattice constant in graphene, the scattering between K and K' points in the Brillouin zone is suppressed and we can assume homogeneous broadening of the LLs.²² The latter can be incorporated into evolution equation for $\rho_{n_1, n_2}(t)$ by the damping term $-i\Gamma_{n_1, n_2} \rho_{n_1, n_2}(t)$ and from Heisenberg equation one can obtain evolution equation for the reduced single-particle density matrix:

$$i\hbar \frac{\partial \rho_{n_1, n_2}(t)}{\partial t} = [\varepsilon_{n_1} - \varepsilon_{n_2}] \rho_{n_1, n_2}(t) - i\Gamma_{n_1, n_2} \rho_{n_1, n_2}(t) - E(t) \sum_n [\mathcal{D}_{n, n_2} \rho_{n_1, n}(t) - \mathcal{D}_{n_1, n} \rho_{n, n_2}(t)]. \quad (12)$$

For the norm-conserving damping matrix we take $\Gamma_{n_1, n_2} = \Gamma(1 - \delta_{n_1, n_2})$, where Γ measures the Landau level broadening.

III. COHERENT NONLINEAR OPTICAL RESPONSE

Solving Eq. (12) with the initial condition (10) one can reveal nonlinear response of the graphene QHE system to a strong laser radiation. At that one can expect intense radiation of harmonics of the incoming wavefield in the result of the coherent transitions between LLs. The harmonics will be described by the additional generated fields $E_{x,y}^{(g)}$. We assume that the generated fields are considerably smaller than the incoming field $|E_{x,y}^{(g)}| \ll |E|$. In this case we do not need to solve self-consistent Maxwell's wave equation with Heisenberg equations. To determine the electromagnetic field of harmonics we can solve Maxwell's wave equation in the propagation direction with the given source term:

$$\frac{\partial^2 E_{x,y}^{(t)}}{\partial z^2} - \frac{1}{c^2} \frac{\partial^2 E_{x,y}^{(t)}}{\partial t^2} = \frac{4\pi}{c^2} \frac{\partial \mathcal{J}_{x,y}(t)}{\partial t} \delta(z). \quad (13)$$

Here $\delta(z)$ is the Dirac delta function, $E_{x,y}^{(t)}$ is the total field, and $\mathcal{J}_{x,y}(t)$ is the mean value of the surface current density operator:

$$\begin{aligned} \hat{\mathcal{J}}_x(t) &= -\frac{e\nu_F g_s g_v}{\mathcal{S}} \langle \hat{\Psi} | \sigma_x | \hat{\Psi} \rangle, \\ \hat{\mathcal{J}}_y(t) &= -\frac{e\nu_F g_s g_v}{\mathcal{S}} \langle \hat{\Psi} | \sigma_y | \hat{\Psi} \rangle. \end{aligned} \quad (14)$$

Here $g_s = 2$ and $g_v = 2$ are the spin and valley degeneracy factors, respectively. With the help of Eqs. (5) and (9), the expectation value (14) of the total current in components can be written in the following form:

$$\begin{aligned} \mathcal{J}_x &= -\frac{e\nu_F}{\pi l_B^2} \sum_{n, n'} \rho_{n', n} (\varkappa_{n, n'} \delta_{|n|, |n'|+1} + \varkappa_{n', n} \delta_{|n|, |n'|-1}), \\ \mathcal{J}_y &= -\frac{ie\nu_F}{\pi l_B^2} \sum_{n, n'} \rho_{n', n} (\varkappa_{n', n} \delta_{|n|, |n'|-1} - \varkappa_{n, n'} \delta_{|n|, |n'|+1}). \end{aligned} \quad (15)$$

In Eq. (15) we have also made summation over the quantum number m which yields the degeneracy factor $\mathcal{S}/2\pi l_B^2$. The solution to equation (13) reads

$$E_{x,y}^{(t)}(t, z) = E_{x,y}(t - z/c) - \frac{2\pi}{c} [\theta(z) \mathcal{J}_{x,y}(t - z/c) + \theta(-z) \mathcal{J}_{x,y}(t + z/c)], \quad (16)$$

where $\theta(z)$ is the Heaviside step function with $\theta(z) = 1$ for $z \geq 0$ and zero elsewhere. The first term in Eq. (16) is the incoming wave. In the second line of Eq. (16), we see that after the encounter with the graphene sheet two propagating waves are generated. One traveling in the propagation direction of the incoming pulse and one traveling in the opposite direction. The Heaviside functions ensure that the generated light propagates from the source located at $z = 0$. We assume that the spectrum is measured at a fixed observation point in the forward propagation direction. For the generated field at $z > 0$ we have

$$E_{x,y}^{(g)}(t - z/c) = -\frac{2\pi}{c} \mathcal{J}_{x,y}(t - z/c). \quad (17)$$

Now, performing the summation in Eqs. (15) and using solutions (17) we can calculate the harmonic radiation spectrum with the help of Fourier transform of the functions $E_{x,y}^{(g)}(t - z/c)$:

$$E_{x,y}^{(g)}(s) = \frac{\omega}{2\pi} \int_0^{2\pi/\omega} E_{x,y}^{(g)}(t) e^{is\omega t} dt = -\frac{2\pi}{c} \mathcal{J}_{x,y}^{(s)}, \quad (18)$$

where

$$\mathcal{J}_{x,y}^{(s)} = \frac{\omega}{2\pi} \int_0^{2\pi/\omega} \mathcal{J}_{x,y}(t) e^{is\omega t} dt. \quad (19)$$

Let us now introduce generalized magneto-optical conductivity of graphene

$$\Sigma_{xx}^{(s)}(\omega, E_0) = \frac{\mathcal{J}_x^{(s)}}{E_x^{(1)}} = \frac{2\mathcal{J}_x^{(s)}}{E_0}, \quad (20)$$

$$\Sigma_{yx}^{(s)}(\omega, E_0) = \frac{\mathcal{J}_y^{(s)}}{E_x^{(1)}} = \frac{2\mathcal{J}_y^{(s)}}{E_0}. \quad (21)$$

Note that in the limit $E_0 \rightarrow 0$ at $s = 1$, from the generalized conductivity (20) and (21) one can derive magneto-optical conductivity of graphene obtained within the framework of linear response theory:

$$\Sigma_{xx}^{(1)}(\omega, E_0 \rightarrow 0) = \sigma_{xx}(\omega), \quad (22)$$

$$\Sigma_{yx}^{(1)}(\omega, E_0 \rightarrow 0) = \sigma_{yx}(\omega). \quad (23)$$

For $s \neq 1$ the quantities defined via Eqs. (20) and (21) describe nonlinear response of the graphene QHE via radiation of harmonics. In the following the nonlinear effects on the fundamental harmonic with limiting linear

case and on the third harmonic will be considered separately.

A. Linear magneto-optical conductivity of graphene

For the comparison with the nonlinear case and for completeness in this subsection we consider magneto-optical conductivity of graphene in the scope of linear response theory. Thus, we first solve Eq. (12) in the first order over the field $E(t)$. We look for the solution of Eq. (12) in the form

$$\rho_{n_1, n_2}(t) \simeq \rho_{n_1, n_2}^{(0)} + \rho_{n_1, n_2}^{(1)},$$

with

$$\rho_{n_1, n_2}^{(0)}(t) = \rho_F(n_1) \delta_{n_1, n_2}.$$

Keeping only first order over $E(t)$ terms from Eq. (12) one can obtain the solution

$$\rho_{n_1, n_2}^{(1)}(t) = \frac{\mathcal{D}_{n_1, n_2} [\rho_F(n_1) - \rho_F(n_2)] E_0 e^{i\omega t}}{\varepsilon_{n_1} - \varepsilon_{n_2} + \hbar\omega - i\Gamma} \frac{1}{2} + \frac{\mathcal{D}_{n_1, n_2} [\rho_F(n_1) - \rho_F(n_2)] E_0 e^{-i\omega t}}{\varepsilon_{n_1} - \varepsilon_{n_2} - \hbar\omega - i\Gamma} \frac{1}{2}, \quad (24)$$

where we have assumed adiabatic turn on of the field $E_0(t \rightarrow 0) = 0$. The magneto-optical conductivity of graphene corresponding to obtained density matrix (24), according to Eqs. (20)-(23) will be given by formulas:

$$\sigma_{xx}(\omega) = -\frac{e^2 i}{h} \frac{1}{2} \sum_{n_1, n_2} \frac{\rho_F(n_1) - \rho_F(n_2)}{\varepsilon_{n_1} - \varepsilon_{n_2} + \hbar\omega - i\Gamma} \left[(1 + \delta_{n_2, 0}) \delta_{|n_1|, |n_2|+1} + (1 + \delta_{n_1, 0}) \delta_{|n_1|, |n_2|-1} \right] \frac{\hbar^2 \omega_B^2}{\varepsilon_{n_2} - \varepsilon_{n_1}}, \quad (25)$$

$$\sigma_{yx}(\omega) = \frac{e^2}{h} \frac{1}{2} \sum_{n_1, n_2} \frac{\rho_F(n_1) - \rho_F(n_2)}{\varepsilon_{n_1} - \varepsilon_{n_2} + \hbar\omega - i\Gamma} \left[(1 + \delta_{n_2, 0}) \delta_{|n_1|, |n_2|+1} - (1 + \delta_{n_1, 0}) \delta_{|n_1|, |n_2|-1} \right] \frac{\hbar^2 \omega_B^2}{\varepsilon_{n_2} - \varepsilon_{n_1}}, \quad (26)$$

where $h = 2\pi\hbar$. Note that Eqs. (25) and (26) for longitudinal ($\sigma_{xx}(\omega)$) and Hall ($\sigma_{yx}(\omega)$) conductivities coincide with results of Ref. [13] obtained via a Green's function calculation and, also, with a Kubo formula calculation within the Dirac cone approximation.¹⁷ The variation of conductivity with the Fermi energy reveals characteristic feature of 2D systems: Hall quantization - when Fermi energy passes through Landau levels. The Hall conductivity quantization rule for graphene can be obtained from Eq. (26). In the limit of $\{\hbar\omega, \Gamma, T\} \ll \hbar\omega_B$ the expression (26) simplifies to

$$\sigma_{yx}(0) = 4 \frac{e^2}{h} \left(n_F + \frac{1}{2} \right), \quad (27)$$

the so-called half-integer quantum Hall quantization rule for graphene⁴ (n_F is the index of the last occupied LL). In Fig. 1 we display linear optical response of graphene QHE system via real part of Hall conductivity (26) versus Fermi energy for various frequencies. The LL broadening is taken to be $\Gamma = 0.1\hbar\omega_B$. As is seen from this figure the Hall conductivity quantization rule persist for low frequency radiation,^{11,17} however for higher frequencies it disappears.

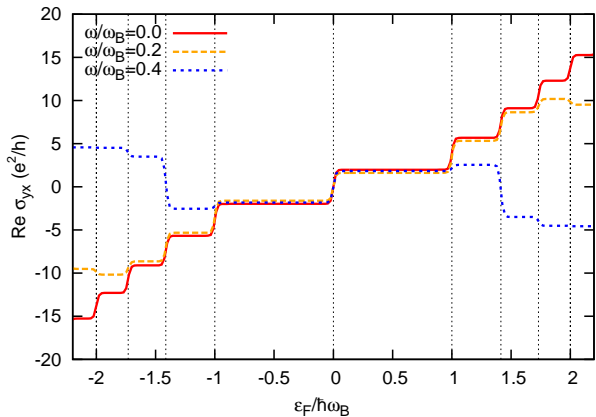


FIG. 1: Linear optical response of graphene QHE system via real part of the Hall conductivity versus Fermi energy for various frequencies. The LL broadening is taken to be $\Gamma = 0.1\hbar\omega_B$. Vertical dashed lines indicate Landau levels.

B. Non-linear magneto-optical conductivity of graphene

For the strong fields Eq. (12) can not be solved analytically and one should use numerical methods. For this propose the time evolution of system (12) is found with the help of the standard fourth-order Runge-Kutta algorithm and for calculation of Fourier transform of the functions $\mathcal{J}_{x,y}(t)$ the fast Fourier transform algorithm is used. For all calculations the temperature is taken to be $T/\hbar\omega_B = 0.01$.

Figures 2 and 3 show nonlinear response of the graphene QHE system via real and absolute value of non-linear optical Hall conductivity versus Fermi energy for various pump wave intensities. From these figures we immediately notice a step-like structure of the non-linear optical Hall conductivity as a function of ε_F for various pump wave intensities. In these figures the vertical dashed lines indicate Landau levels. Although the step heights are not quantized exactly, the flatness, which is an intrinsic property of the static QHE, surprisingly exists also in the nonlinear response of the graphene. In the static QHE the step structure of the Hall conductivity is a quantum and topological effect. In the considered case Eqs. (15) does not simply reduce to a topological expression and the result for the robust plateaus of the non-linear optical response is nontrivial. We further examine how the step-like structure in the nonlinear response of the graphene behaves for various pump wave frequencies. Absolute value of non-linear optical Hall conductivity of graphene QHE system at the fundamental harmonic is shown in Fig. 4. Thus, the step structure preserves for the wide range of the pump wave frequencies.

We also examine how the step-like structure in the non-linear optical response of graphene QHE system behaves as we vary the LL broadening. So we have calculated $\Sigma_{yx}^{(1)}$ as a function of Γ , for fixed values of ω and χ . We can

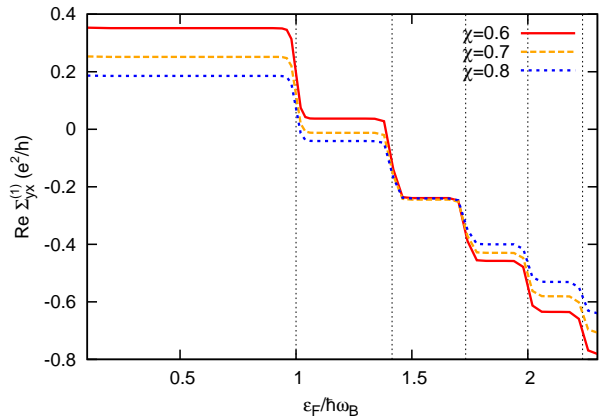


FIG. 2: Real part of non-linear optical Hall conductivity of graphene QHE system versus Fermi energy for various pump wave intensities with $\omega = 0.5\omega_B$. The LL broadening is taken to be $\Gamma = 0.2\hbar\omega_B$.

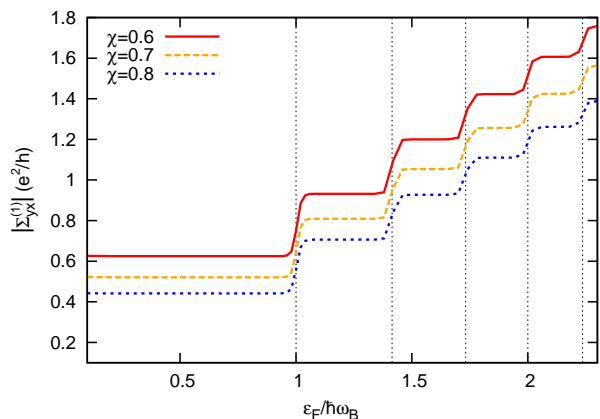


FIG. 3: Absolute value of non-linear optical Hall conductivity of graphene QHE system versus Fermi energy for various pump wave intensities with $\omega = 0.5\omega_B$. The LL broadening is taken to be $\Gamma = 0.2\hbar\omega_B$.

see from Fig. 5 that, while the density of states broadens with a width $\sim \Gamma$ the step structure remains up to large Γ . Note that the non-linear optical Hall conductivity of graphene QHE as in the case of linear response case defines Faraday rotation and ellipticity of the transmitted wave. It is straightforward from Eqs. (18) and (21) that generated field on the fundamental harmonic polarized perpendicular to the polarization of a pump wave is defined as

$$E_y^{(g)} = -\frac{2\pi E_0}{c} \left(\text{Re}\Sigma_{yx}^{(1)} \cos\omega t - \text{Im}\Sigma_{yx}^{(1)} \sin\omega t \right). \quad (28)$$

Hence, the absolute value of Faraday rotation angle (ϑ_F) and ellipticity (δ_F) will be defined as:

$$|\vartheta_F| = \frac{2\pi}{c} \left| \text{Re}\Sigma_{yx}^{(1)} \right|; \quad |\delta_F| = \frac{2\pi}{c} \left| \text{Im}\Sigma_{yx}^{(1)} \right|. \quad (29)$$

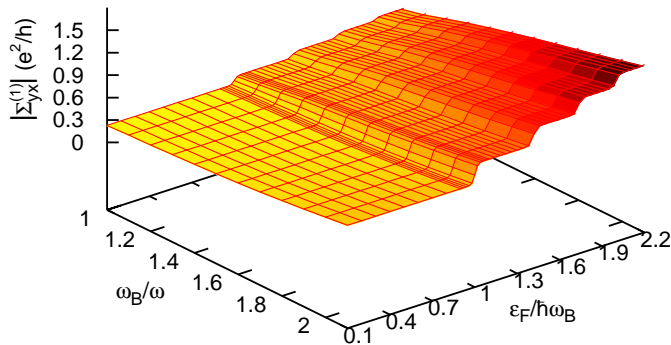


FIG. 4: Absolute value of non-linear optical Hall conductivity of graphene QHE system versus Fermi energy and pump wave frequency (ratio ω_B/ω) for a wave of intensity $\chi = 0.8$. The LL broadening is taken to be $\Gamma = 0.2\hbar\omega_B$.

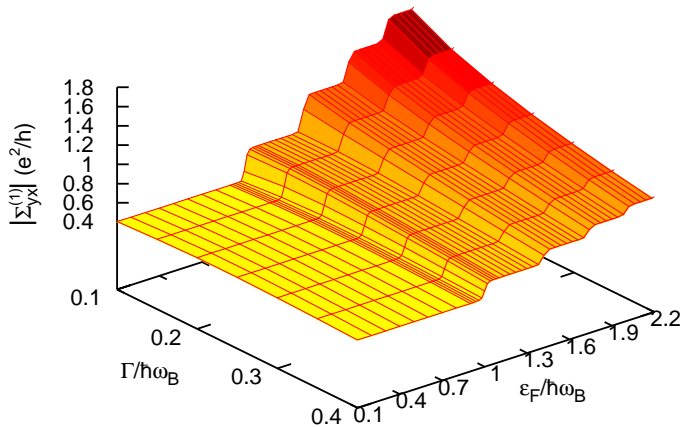


FIG. 5: Absolute value of non-linear optical Hall conductivity of graphene QHE system versus Fermi energy and LL broadening for a wave of intensity $\chi = 0.8$ and frequency $\omega = 0.5\omega_B$.

Thus, Faraday rotation angle and ellipticity present a step-like structure as the Fermi energy crosses different Landau levels.

C. Third harmonic radiation process

The nonlinear response of the graphene QHE system to a strong laser radiation is also proceeded by radiation of harmonics of the incoming wave-field in the result of the coherent transitions between LLs. As is seen from

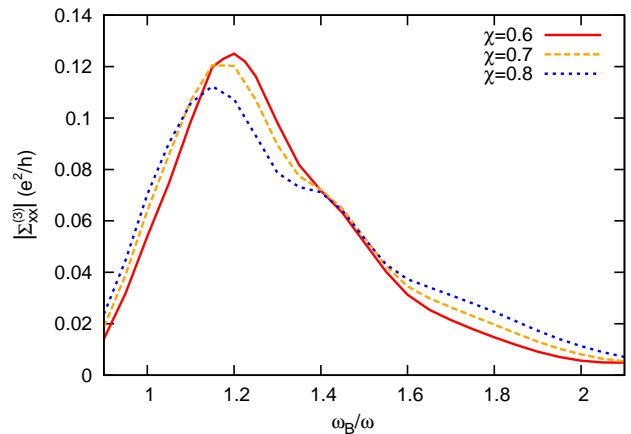


FIG. 6: Generalized longitudinal magneto-optical conductivity of graphene QHE on the third harmonic of a pump wave versus ratio ω_B/ω for various intensities at $\varepsilon_F/\hbar\omega_B = 0.5$. The LL broadening is taken to be $\Gamma = 0.2\hbar\omega_B$.

Eqs. (12) and (15), the spectrum contains in general both even and odd harmonics. However, depending on the initial conditions, in particular, for the equilibrium initial state (10) and at the smooth turn-on-off of the wave field the terms containing even harmonics cancel each other because of inversion symmetry of the system and only the odd harmonics are generated. The emission strength of the s th harmonic is characterized by the generalized magneto-optical conductivity of graphene $\Sigma_{xx}^{(s)}$ and $\Sigma_{yx}^{(s)}$. Calculations show that for $s > 1$ $|\Sigma_{xx}^{(s)}| \gg |\Sigma_{yx}^{(s)}|$, that is harmonics are radiated with the same polarization as incoming wave. Hence, we will consider moderately strong waves and we confine ourselves to only third harmonic radiation process and numerically investigate generalized longitudinal magneto-optical conductivity of graphene QHE on the third harmonic $\Sigma_{xx}^{(3)}$. To determine optimal values of a pump wave frequency for third harmonic radiation process we calculated $\Sigma_{xx}^{(3)}$ as a function of a pump wave frequency for various intensities (Fig. 6). As is seen optimal frequencies are close to the cyclotron frequency ω_B .

Then we investigate the variation of conductivity $\Sigma_{xx}^{(3)}$ with the Fermi energy. In Fig. 7 the third harmonic radiation strength in graphene QHE system via absolute value of generalized longitudinal conductivity versus Fermi energy for various pump wave intensities is shown. From these figure we also notice a step-like structure of the generalized longitudinal magneto-optical conductivity on the third harmonic. However, $|\Sigma_{xx}^{(3)}|$ decreases with the increase of the Fermi energy, which is connected with the fact that due to nonequidistant Landau levels in graphene the transitions with large energy difference give main contribution to $\Sigma_{xx}^{(3)}$ for this frequency range and with the increase of Fermi energy because of Pauli

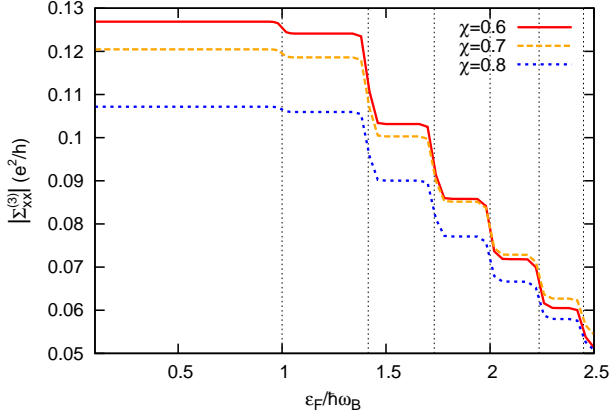


FIG. 7: The third harmonic radiation strength in graphene QHE system via absolute value of generalized longitudinal conductivity versus Fermi energy for various pump wave intensities with $\omega_B = 1.2\omega$. The LL broadening is taken to be $\Gamma = 0.2\hbar\omega_B$.

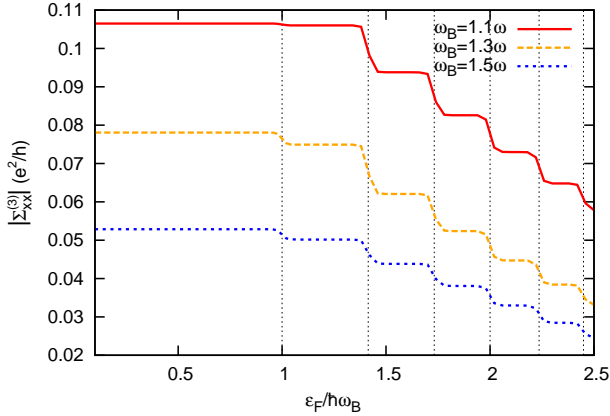


FIG. 8: The third harmonic radiation strength in graphene QHE system via absolute value of generalized longitudinal conductivity versus Fermi energy for various pump wave frequencies with $\chi = 0.8$. The LL broadening is taken to be $\Gamma = 0.2\hbar\omega_B$.

blocking the contribution of these transitions are vanished.

We also examine how the step-like structure in the $\Sigma_{xx}^{(3)}$ behaves depending on the pump wave frequency and LL broadening. The results of our calculations are shown in Figs. (8) and (9). Thus, the step structure preserves for large LL broadening and for the wide range of the pump wave frequencies.

IV. DISCUSSION AND SUMMARY

Finally let us consider the experimental feasibility of considered processes. It is clear that in experiment one can observe the considered effect by measuring $\Sigma_{yx}^{(1)}$

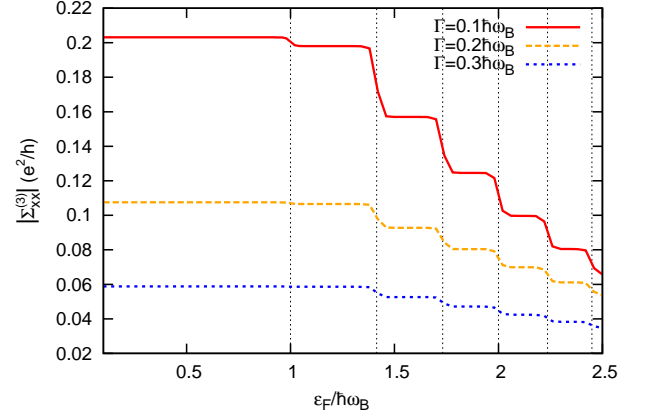


FIG. 9: The third harmonic radiation strength in graphene QHE system via absolute value of generalized longitudinal conductivity versus Fermi energy for various values of LL broadening at fixed pump wave frequency $\omega = 1.1\omega_B$. The intensity parameter is taken to be $\chi = 0.7$.

and/or $\Sigma_{xx}^{(3)}$. The first quantity is responsible for the nonlinear Faraday effect, while last quantity responsible for third harmonic radiation polarized along the incoming wave polarization. Thus, the step structure should be observed as jumps in the intensity of third harmonic ($I_x^{(3)}$) or fundamental harmonic radiation with orthogonal polarization ($I_y^{(1)}$). These quantities are proportional to the pump wave intensity (I). From Eqs. (18), (20), and (21)) it follows that $I_x^{(3)} = \alpha^2 I \left| \Sigma_{xx}^{(3)} h/e^2 \right|^2$ and $I_y^{(1)} = \alpha^2 I \left| \Sigma_{yx}^{(1)} h/e^2 \right|^2$, where α is the fine structure constant. For the pump wave field we will assume a CO₂ laser with $\hbar\omega \simeq 0.1$ eV. The average intensity of the wave for $\chi = 0.8$ is $I \simeq 5 \times 10^7$ W/cm². For the setup of Fig. 7 with the chosen parameters the average intensity of the third harmonic radiation on the first plateau is $I_x^{(3)} \simeq 30$ W/cm² and the first step is $\Delta I_x^{(3)} \sim 10$ W/cm². For the setup of Fig. 4 the average intensity on the first plateau is $I_y^{(1)} \simeq 180$ W/cm² and the first step is $\Delta I_y^{(1)} \sim 280$ W/cm². Thus, that the present effect is well within the experimental feasibility.

To summarize, we have presented a microscopic theory of the graphene interaction with coherent electromagnetic radiation in the quantum Hall regime. The evolutionary equation for a single-particle density matrix has been solved numerically. We have revealed that the nonlinear optical response of graphene to a strong laser radiation in the quantum Hall regime, in particular, radiation strength on the third harmonics, as well as nonlinear Faraday effect, has a characteristic Hall plateau structures that persist for a wide range of the pump wave frequencies and intensities even for significant broadening of LLs because of impurities in graphene.

Acknowledgments

No. 15T-1C013.

This work was supported by the RA MES State Committee of Science, in the frames of the research project

-
- ¹ K. S. Novoselov, A. K. Geim, S. V. Morozov, D. Jiang, Y. Zhang, S. V. Dubonos, I. V. Grigorieva, and A. A. Firsov, *Science* **306**, 666 (2004).
- ² A. H. Castro Neto, F. Guinea, N. M. R. Peres, K. S. Novoselov, and A. K. Geim, *Rev. Mod. Phys.* **81**, 109 (2009).
- ³ H. K. Avetissian, A. K. Avetissian, G. F. Mkrtchian, Kh. V. Sedrakian, *Phys. Rev. B* **85**, 115443 (2012); *J. Nanophoton.* **6**, 061702 (2012).
- ⁴ K. S. Novoselov *et al.*, *Nature* **438**, 197 (2005).
- ⁵ Y. Zhang *et al.*, *Nature* **438**, 201 (2005).
- ⁶ V. P. Gusynin and S. G. Sharapov, *Phys. Rev. Lett.* **95**, 146801 (2005).
- ⁷ M. O. Goerbig, *Rev. Mod. Phys.* **83**, 1193 (2011).
- ⁸ K. v. Klitzing, G. Dorda, and M. Pepper, *Phys. Rev. Lett.* **45**, 494 (1980).
- ⁹ D. J. Thouless, M. Kohmoto, M. P. Nightingale, and M. den Nijs, *Phys. Rev. Lett.* **49**, 405 (1982).
- ¹⁰ Y. Hatsugai, T. Fukui, and H. Aoki, *Phys. Rev. B* **74**, 205414 (2006).
- ¹¹ T. Morimoto, Y. Hatsugai, and H. Aoki, *Phys. Rev. Lett.* **103**, 116803 (2009).
- ¹² N. M. R. Peres, F. Guinea, and A. H. Castro Neto, *Phys. Rev. B* **73**, 125411 (2006).
- ¹³ V. P. Gusynin, S. G. Sharapov, and J. P. Carbotte, *Phys. Rev. Lett.* **98**, 157402 (2007); *Int. Jour. of Mod. Phys. B* **21**, 4611 (2007).
- ¹⁴ C. Zhang, L. Chen, and Z. S. Ma, *Phys. Rev. B* **77**, 241402 (2008).
- ¹⁵ C. H. Yang, F. M. Peeters, and W. Xu, *Phys. Rev. B* **82**, 205428 (2010).
- ¹⁶ T. Morimoto, Y. Hatsugai, and H. Aoki, *Phys. Rev. B* **78**, 073406 (2008).
- ¹⁷ A. Ferreira, J. Viana-Gomes, Yu. V. Bludov, V. Pereira, N. M. R. Peres, and A. H. Castro Neto, *Phys. Rev. B* **84**, 235410 (2011).
- ¹⁸ F. Wendler, A. Knorr, E. Malic, *Nature Commun.* **5** 3703 (2014).
- ¹⁹ F. Wendler, A. Knorr, E. Malic, *Nanophotonics* **4**, 224 (2015).
- ²⁰ F. Wendler, E. Malic, *Scientific Reports* **5**, 12646 (2015).
- ²¹ H. K. Avetissian, G. F. Mkrtchian, K. G. Batrakov, S. A. Maksimenko, A. Hoffmann, *Phys. Rev. B* **88**, 245411 (2013); *Phys. Rev. B* **88**, 165411 (2013).
- ²² N. H. Shon and T. Ando, *J. Phys. Soc. Jpn.* **67**, 2421 (1998).